A Complex Variable Perturbed Gauss-Newton Method for Tracking Mode State Estimation

Izudin Džafić, *Senior Member, IEEE*, Rabih A. Jabr, *Fellow, IEEE*, and Tarik Hrnjić, *Student Member, IEEE*

***Abstract*—The recent power systems literature has witnessed an intensified interest in state estimation methods that can handle a vast array of measurements from large-scale networks while maintaining performance that is commensurate with real-time requirements. When measurements are from the Supervisory Control and Data Acquisition (SCADA) system and Phasor Measurement Units (PMUs), an elegant formulation of the weighted least squares problem can be cast in complex variables and solved via the Gauss-Newton (GN) method. This paper presents a Perturbed Gauss-Newton (PGN) method in complex variables that is suitable for real-time tracking of the network's state vector. The proposed PGN method is built around an entirely linear measurement model expressed in function of the complex phasor voltages, and its iterative solution scheme requires one factorization of the coefficient matrix followed by repeated forward/backward substitutions. The complex variable PGN method for state estimation can be therefore seen as the counterpart of the classical implicit bus impedance method for power flow. The paper reports numerical results of the PGN method on large-scale transmission networks having up to 9241 nodes and contrasts the proposed method with the equality constrained GN method in complex variables and a recent two-stage estimator also operating in the complex domain.**

***Index Terms*—Iterative algorithms, least squares approximation, optimization methods, perturbation methods, state estimation.**

I. Introduction

THE proliferation of Phasor Measurement Units (PMUs) in transmission networks has been coupled with the development of linear state estimation methods employing phasor only measurements [1], and a practical implementation of such an estimator has been running in the 500 kV system of Pacific Gas & Electric (PG&E) [2]. However, the majority of transmission network state estimators worldwide still employ measurements from the Supervisory Control and Data Acquisition (SCADA) system in addition to PMUs. In this case, a hybrid state estimator is used to compute the network state from both the legacy SCADA and PMU measurements [3]. The requirements of regional electricity markets in terms of observing long-distance energy transactions translate into a broader geographical scope of state estimation [4]. The associated rise in the number of measurements has fueled research into hybrid state estimation methods that efficiently estimate large scale networks [5]. The approaches that achieve speed-up belong to the family of constant gain matrix estimators [6], [7] that are executed in tracking mode, i.e., when there are no changes in the network topology and in the measurement weights. This paper proposes a constant gain matrix hybrid estimator operating entirely in complex variables and derived via the perturbed Gauss-Newton method [8] and Wirtinger calculus [9], [10]. The resulting approach can be viewed as an extension of the implicit Z-bus power flow method, as described in [11], [12], to state estimation.

The linear state estimators employing only PMU measurements employ either the weighted least squares (WLS) [13] or the weighted least absolute value (WLAV) [14] objective function for better bad data rejection. The linear WLS method can be written in a decoupled form [15] and using complex variables [16]. While the linear WLS state estimators are non-iterative, the hybrid WLS estimators require several iterations, each of which entails matrix factorization [17], [18]. From a computational perspective, there have been several advances even before the development of hybrid estimation methodologies. A significant contribution is the fast decoupled state estimator [19], [20] that was used in AEP's control center in 1982 [21]. The convergence of the decoupled estimator, however, weakens when the transmission lines have low X/R ratios, and the decoupled version is not preferable over conventional WLS when current magnitudes form part of the measurement set [19]. Although current magnitude measurements are seldom utilized in transmission state estimation, they could be useful to achieve observability at the sub-transmission level [22]. The limitations of the decoupled estimator have motivated the development of bilinear state estimation [22], which is essentially a three-stage solution method that involves two linear WLS solutions and an intermediate nonlinear transformation; the last stage needs high redundancy so that the extended state vector remains observable. Subsequent extensions to the bilinear state estimator include the equality constrained formulation to handle virtual measurements [23] and the mixed-integer linear programming model for robust state estimation [24]. Another interesting non-iterative state estimator employs the Kipnis-Shamir re-linearization technique to solve an over-determined system of polynomial equations [25]–[27]; its last phase for extracting the state vector necessitates special care to avoid nonphysical solutions. Other

Manuscript received June 1, 2020; revised September 16, 2020; accepted October 25, 2020. Date of publication October 28, 2020; date of current version April 19, 2021. Paper no. TPWRS-00905-2020. *(Corresponding author: Izudin Džafić.)*

Izudin Džafić and Tarik Hrnjić are with the Faculty of Electrical Engineering, University of Sarajevo, Sarajevo 71000, Bosnia and Herzegovina (e-mail: idzafic@ieee.org; thrnjic@etf.unsa.ba).

Rabih A. Jabr is with the Department of Electrical, and Computer Engineering, American University of Beirut, Beirut 1107 2020, Lebanon (e-mail: rabih.jabr@aub.edu.lb).

Color versions of one or more of the figures in this article are available online at https://ieeexplore.ieee.org.

Digital Object Identifier 10.1109/TPWRS.2020.3034371

recent approaches include a linear hybrid estimator that uses an equivalent circuit model whose component parameters are inferred from measurements [28]–[30] and a two-stage linear state estimator in complex variables [5]. The literature review shows a trend in state estimation research that principally targets fast solution

This paper proposes a new constant gain matrix method for hybrid state estimation operating entirely in the complex domain. The constant gain matrix is systematically derived from the perturbed Gauss-Newton method for nonlinear least-squares by using Wirtinger calculus [9], [10], in contrast to real variable calculus as initially reported in [8]. The decoupling between the complex state vector and its conjugate is obtained by turning SCADA measurements into equivalent phasor measurements. The resulting constant gain matrix iterative scheme is equivalent to extending the implicit Z-bus power flow method [11], [12] to hybrid state estimation, in a manner that parallels the extension of the fast decoupled power flow [31] to fast decoupled state estimation [19], [20]. The proposed decoupled implementation is suited to tracking mode operation and has been contrasted with the recent complex variable two-stage linear state estimator [5].

The rest of this paper is organized as follows. Section II presents the derivation of the perturbed Gauss-Newton method in complex variables and the decoupling principle. Section III describes the decoupled implementation of the hybrid state estimator, including the incorporation of equality constraints to handle virtual measurements. Bad data detection and identification are detailed in Section IV . Section V reports numerical results on large scale networks having up to 9241 nodes in addition to comparison with [5]. The paper is concluded in Section VI.

II. Decoupled and Perturbed Gauss-Newton Method in Complex Variables

A. Gauss-Newton Method

Consider the nonlinear weighted least squares problem in complex variables:

$$\min_{(x,\overline{x})}\phi(x,\overline{x}) = \frac{1}{2}\overline{f}^T(x,\overline{x})W_M f(x,\overline{x}) \tag{1}$$

where x is an n-dimensional complex vector, f is an m-dimensional complex vector function of x and $\overline{x}$, the bar sign denotes complex conjugation, and W_M is a diagonal weighting matrix. The vector function f is partitioned into an $m_c \times 1$ vector f_c of complex functions and its conjugate $\overline{f}_c$:

$$f(x,\overline{x}) = \begin{bmatrix} f_c(x,\overline{x}) \\ \overline{f}_c(x,\overline{x}) \end{bmatrix} \tag{2}$$

The problem in (1) can be therefore written as:

$$\min_{(x,\overline{x})}\phi(x,\overline{x}) = \sum_{i=1}^{m_c} w_i \overline{f}_{ci} f_{ci} \tag{3}$$

The gradient of $\phi(x,\overline{x})$ is given by:

$$F(x,\overline{x}) = \nabla_{(\overline{x},x)}\phi(x,\overline{x}) = \overline{J}^T(x,\overline{x})W_M f(x,\overline{x}) \tag{4}$$

where:

$$J(x,\overline{x}) = \begin{bmatrix} J_{cx} & J_{c\overline{x}} \\ \overline{J}_{c\overline{x}} & \overline{J}_{cx} \end{bmatrix} \tag{5}$$

J_{cx} and $J_{c\overline{x}}$ are the Jacobian and conjugate Jacobian matrices of f_c:

$$J_{cx} = \begin{bmatrix} \frac{\partial f_{c1}}{\partial x_1} & \cdots & \frac{\partial f_{c1}}{\partial x_n} \\ \vdots & & \vdots \\ \frac{\partial f_{c(m_c)}}{\partial x_1} & \cdots & \frac{\partial f_{c(m_c)}}{\partial x_n} \end{bmatrix} \tag{6}$$

$$J_{c\overline{x}} = \begin{bmatrix} \frac{\partial f_{c1}}{\partial \overline{x}_1} & \cdots & \frac{\partial f_{c1}}{\partial \overline{x}_n} \\ \vdots & & \vdots \\ \frac{\partial f_{c(m_c)}}{\partial \overline{x}_1} & \cdots & \frac{\partial f_{c(m_c)}}{\partial \overline{x}_n} \end{bmatrix} \tag{7}$$

The classical Gauss-Newton algorithm is defined in the steps below:

Step 1: Initialize the iteration counter ($k = 1$) and the initial solution $x^{(1)}$.

Step 2: Compute $J(x^{(k)},\overline{x}^{(k)})$ and form the gain matrix:

$$G(x^{(k)},\overline{x}^{(k)}) = \overline{J}^T(x^{(k)},\overline{x}^{(k)})W_M J(x^{(k)},\overline{x}^{(k)}) \tag{8}$$

Factorize $G(x^{(k)},\overline{x}^{(k)})$ using Cholesky decomposition.

Step 3: Compute $f(x^{(k)},\overline{x}^{(k)})$ and form the right-hand-side:

$$\beta(x^{(k)},\overline{x}^{(k)}) = -\overline{J}^T(x^{(k)},\overline{x}^{(k)})W_M f(x^{(k)},\overline{x}^{(k)}) \tag{9}$$

Step 4: Solve the complex normal equations using the Cholesky factors and Forward/Backward substitution:

$$G(x^{(k)},\overline{x}^{(k)}) \begin{bmatrix} \Delta x^{(k)} \\ \Delta \overline{x}^{(k)} \end{bmatrix} = \beta(x^{(k)},\overline{x}^{(k)}) \tag{10}$$

Step 5: Update the solution vector and its conjugate:

$$\begin{bmatrix} x^{(k+1)} \\ \overline{x}^{(k+1)} \end{bmatrix} = \begin{bmatrix} x^{(k)} \\ \overline{x}^{(k)} \end{bmatrix} + \begin{bmatrix} \Delta x^{(k)} \\ \Delta \overline{x}^{(k)} \end{bmatrix} \tag{11}$$

Step 6: If $|\Delta x^{(k)}|_\infty < \varepsilon$, stop and print the solution. Otherwise, update the iteration counter ($k \leftarrow k+1$) and go to Step 2.

B. Perturbed Gauss-Newton Method

In the perturbed Gauss-Newton method [8], $J(x,\overline{x})$ in (5) is replaced by an approximation $\tilde{J}(x,\overline{x})$ that is easier to compute and makes it cheaper to solve the normal equations. When the computation is carried out using real variables, Ref. [8] gives explicit conditions on the perturbed Jacobian that are sufficient to guarantee convergence. In essence, the conditions state that the gain matrix $\tilde{G}(x,\overline{x}) = \overline{\tilde{J}}^T(x,\overline{x})W_M\tilde{J}(x,\overline{x})$ is a good approximation to the derivative of the perturbed gradient equation:

$$\tilde{F}(x,\overline{x}) = \overline{\tilde{J}}^T(x,\overline{x})W_M f(x,\overline{x}) \tag{12}$$

In power system computing, it is well known that the power flow Jacobian is rather insensitive to relatively small variations in the solution vector. If the matrix $\tilde{J}(x,\overline{x})$ is set to remain

constant throughout the iterations, then the Cholesky decomposition of $\tilde{G}(x,\overline{x})$ would have to be carried out only once. The perturbed Gauss-Newton algorithm would be the same as in the Gauss-Newton method in Section II-A, except that whenever the stopping criterion is not met, the algorithm resumes iteration at Step 3 with $J(x,\overline{x})$ replaced by its approximation $\tilde{J}(x,\overline{x})$.

C. Perturbed Gauss-Newton Method: Decoupled Implementation

For some applications, it happens that the elements of the conjugate Jacobian of f_c, i.e., $J_{c\overline{x}}$, are relatively smaller than the elements of the Jacobian J_{cx}. In this setting, the approximation $\tilde{J}(x,\overline{x})$ becomes:

$$\tilde{J}(x,\overline{x}) = \begin{bmatrix} \tilde{J}_{cx} & 0 \\ 0 & \overline{\tilde{J}}_{cx} \end{bmatrix} \tag{13}$$

The above equation gives rise to the decoupled normal equations

$$\begin{bmatrix} \overline{\tilde{J}}_{cx}^{T} W \tilde{J}_{cx} & 0 \\ 0 & \tilde{J}_{cx}^{T} W \overline{\tilde{J}}_{cx} \end{bmatrix} \begin{bmatrix} \Delta x^{(k)} \\ \Delta \overline{x}^{(k)} \end{bmatrix} = \begin{bmatrix} -\overline{\tilde{J}}_{cx}^{T} W f_c \\ -\tilde{J}_{cx}^{T} W \overline{f}_c \end{bmatrix} \tag{14}$$

where

$$W_M = \begin{bmatrix} W & 0 \\ 0 & W \end{bmatrix} \tag{15}$$

The block matrix equations in (14) are complex conjugates of each other. Therefore, it is sufficient to solve the normal equations for $\Delta x^{(k)}$:

$$\left[\overline{\tilde{J}}_{cx}^{T} W \tilde{J}_{cx} \right] \Delta x^{(k)} = -\overline{\tilde{J}}_{cx}^{T} W f_c(x^{(k)}, \overline{x}^{(k)}) \tag{16}$$

Eq. (16) requires solving a matrix equation that is half the size of (10).

III. Application to Hybrid State Estimation

Hybrid power system state estimation seeks to estimate the state of the network from measurements obtained via both the SCADA system and PMUs. In the conventional complex variable state estimation [32], the vector of complex measurement residuals is:

$$r(x,\overline{x}) = z_m - h(x,\overline{x}) \tag{17}$$

where z_m is the vector of measurements and $h(x,\overline{x})$ represents a vector of generally nonlinear measurement functions in terms of the complex state vector x and its conjugate $\overline{x}$. The proposed method makes use of the alternative complex measurement residuals given by:

$$f_c(x,\overline{x}) = z_c(x,\overline{x}) - Hx \tag{18}$$

In (18), Hx is a complex valued vector of linear measurement functions in terms of the complex state vector x; Hx represents phasor voltages and branch/injection phasor currents. The complex valued vector $z_c(x,\overline{x})$ of generally nonlinear functions transforms the measurement vector z_m into its equivalent vector phasor measurement that is in function of x and $\overline{x}$. The Appendix includes the details of this transformation.

A. Normal Equations – Perturbed Gauss-Newton Method: Decoupled Implementation

The perturbed Jacobian and conjugate Jacobian matrices of f_c as given by (18) are constant matrices:

$$\tilde{J}_{cx} = -H, \;\; \tilde{J}_{c\overline{x}} = 0 \tag{19}$$

Using (18) and (19) in (16) gives:

$$\left[\overline{H}^{T} W H \right] \left(x^{(k+1)} - x^{(k)} \right) = \overline{H}^{T} W \left(z_c(x^{(k)}, \overline{x}^{(k)}) - H x^{(k)} \right) \tag{20}$$

or

$$\left[\overline{H}^{T} W H \right] x^{(k+1)} = \overline{H}^{T} W z_c(x^{(k)}, \overline{x}^{(k)}) \tag{21}$$

The decoupled implementation of the perturbed Gauss-Newton method is according to the following algorithm:

Step 1: Initialize the iteration counter ($k = 1$) and the initial solution $x^{(1)}$.

Step 2: Compute H and form the reduced gain matrix:

$$G_c = \overline{H}^{T} W H \tag{22}$$

Factorize G_c using Cholesky decomposition.

Step 3: Compute $z_c(x^{(k)}, \overline{x}^{(k)})$ and form the right-hand-side:

$$\beta_c(x^{(k)}, \overline{x}^{(k)}) = \overline{H}^{T} W z_c(x^{(k)}, \overline{x}^{(k)}) \tag{23}$$

Step 4: Solve the complex normal equations using the Cholesky factors and Forward/Backward substitution:

$$G_c x^{(k)} = \beta_c(x^{(k)}, \overline{x}^{(k)}) \tag{24}$$

Step 5: If $|x^{(k+1)} - x^{(k)}|_\infty < \varepsilon$, stop and print the solution. Otherwise, update the iteration counter ($k \leftarrow k+1$) and go to Step 3.

The above procedure is essentially similar to the Z-bus power flow [11], [12], also known as the current injection approach, as it maintains a constant complex valued matrix (22) throughout the iterations while simply updating the right-hand side (23).

Ref. [33] shows that the weighted least-absolute value (WLAV) estimator in real variables has an iteratively reweighted least-squares implementation. It is known that the WLAV estimator is capable of rejecting a wrong data measurement, as long as it is not a leverage point. The iterative scheme in [33] corresponds to solving a sequence of linear weighted least-squares problems. Therefore, the above procedure allows for an iteratively reweighted implementation of the WLAV estimator using the PGN method, but in real variables. Also, the reweighting requires the update and factorization of the gain matrix at every iteration, i.e., the technique would not belong to the category of constant gain matrix methods.

B. Equality Constrained Normal Equations – Perturbed Gauss-Newton Method: Decoupled Implementation

Virtual measurements arise from nodes with zero-injections, i.e., nodes that have neither generation nor load connected at them. Virtual measurements are considered as error-free and are consequently assigned a relatively much higher weight in the normal equations approach; this may result in ill-conditioning

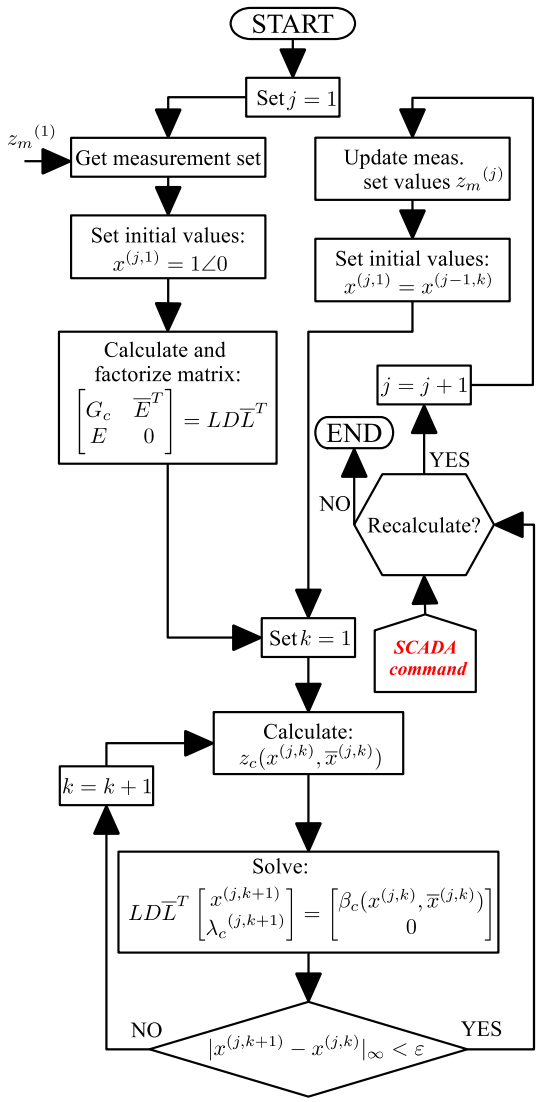

Fig. 1. Flowchart of the tracking mode equality-constrained Perturbed Gauss-Newton Estimator (PGNE).

during the iterative solution process. A better solution is to consider the virtual measurements as phasor current injections that are equal to zero, leading to the equality constrained normal equations:

$$\begin{bmatrix} G_c & \overline{E}^T \\ E & 0 \end{bmatrix} \begin{bmatrix} x^{(k+1)} \\ \lambda_c^{(k+1)} \end{bmatrix} = \begin{bmatrix} \beta_c(x^{(k)}, \overline{x}^{(k)}) \\ 0 \end{bmatrix} \tag{25}$$

When using (25) in the perturbed Gauss-Newton algorithm of Section III-A, Step 2 would require factoring the coefficient matrix in (25) using Bunch Kaufmann decomposition, and Step 4 solves (25) using Forward/Backward substitution. Fig. 1 shows the flowchart of the equality-constrained Perturbed Gauss-Newton Estimator (PGNE) when employed in tracking mode. The index j refers to the time-step number in tracking mode operation. The term equality-constrained is dropped from the PGNE acronym for compactness.

IV. Bad Data Detection and Identification

The ability to detect, identify, and eliminate erroneous measurements is an essential function of the state estimator [34]. This section consists of two parts: bad data detection in Section IV-A, which describes a procedure that determines if the data contains any wrong measurements, and bad data identification in Section IV-B, describing an algorithm that identifies erroneous measurements in the data set. The bad data detection and identification are along the lines in [34], but with the equations updated where necessary to account for the fact that the state vector is complex valued.

A. Bad Data Detection (BDD)

Bad data detection is carried out using the Chi-squares test; the test consists of the following steps:

Step 1: Solve the SE problem to find the state vector estimate $\hat{x}$ and compute the objective function $\phi(\hat{x}, \overline{\hat{x}})$ as given by (3).

Step 2: Compute the number of degrees of freedom Υ, given by the number of measurements minus the number of states, and choose a value for the significance level α, typically in the range 0.01 to 0.05. Given that the probability density for ϕ is chi-squared with Υ degrees of freedom, use the chi-squares table to find t_ϕ, such that the probability that ϕ is greater than t_ϕ is equal to α:

$$\Pr\left(\phi > t_\phi | \, \phi \sim \chi^2(\Upsilon)\right) = \alpha \tag{26}$$

Step 3: Test if:

$$\phi(\hat{x}, \overline{\hat{x}}) > t_\phi \tag{27}$$

If (27) is satisfied, then the presence of bad data will be suspected and the probability that this is a false alarm is α. Otherwise, bad data will not be suspected with a confidence level of $(1-\alpha)$.

B. Bad Data Identification (BDI)

In the case when the chi-squares test detects the existence of bad data in the measurement set, further processing is needed to identify the erroneous measurement. This is accomplished using the Largest Normalized Residual (LNR) test, which consists of the following steps [35]:

Step 1: Compute the measurement residual vector $f_c(\hat{x}, \overline{\hat{x}})$ as given by (18).

Step 2: Calculate diagonal entries of the residual covariance matrix Ω, starting from the Cholesky factors of G_c:

$$G_c = L_c \overline{L}_c^T \tag{28}$$

Step 2.1: Calculate the column entries of temporary matrix T by solving the following system for each row $H_{(i,:)}$ of H:

$$L_c \overline{L}_c^T T_{(:,i)} = \overline{H}_{(i,:)}^T \tag{29}$$

Step 2.2: Compute the diagonal entries of the residual covariance matrix using:

$$\Omega_{ii} = \frac{1}{W_{ii}} - H_{(i,:)} T_{(:,i)} \tag{30}$$

TABLE I
MEASUREMENT COUNT

Net.	Measurement #			
	ZI	S	PMU_I	PMU_V
118A	10	186	186	3
118B	10	0	186	118
1888A	680	2531	1261	87
1888B	680	0	2531	1888
9241A	2901	16049	8025	66
9241B	2901	0	16049	9241

TABLE II
MEASUREMENT STANDARD DEVIATION

	SCADA Measurements			PMU Measurements		
	voltage inj.	power flows		voltage	current	ph. angle
Std. Dev.	2%	2%	2%	0.5%	0.5%	0.1°

Step 3: Compute the elements of the normalized residual vector f_c^n:

$$f_{ci}^n = \frac{|f_c|}{\sqrt{\Omega_{ii}}} \tag{31}$$

Step 4: Find the largest element of the f_c^n vector and compare it to the identification threshold c. If $\max(f_c^n) \geq c$, then the measurement corresponding to the maximum normalized residual is suspected as bad data. Else, stop, no bad data is identified in the measurement set.

Step 5: Eliminate the measurement corresponding to $\max(f_c^n)$ and go to Step 1.

V. NUMERICAL RESULTS

The equality-constrained Perturbed Gauss-Newton Estimator (PGNE) in complex variables (c.f. Fig. 1) was contrasted with:

- the Complex Equality-Constrained Estimator (CECE) in [35]. It is essentially the traditional equality-constrained WLS state estimator [34] but implemented using complex variables.
- the Complex Two-Stage Estimator (CTSE) in [5]. It also employs complex variables and promises fast execution.

The three estimators, i.e., PGNE, CECE, and CTSE, were programmed in C++ and executed on a PC with an Intel i5-7600 K processor and 16 GB of RAM. The comparison was carried out on three networks whose datasets are given with the distribution files of MATPOWER [36], [37]. Table I shows two measurement sets for each system. The table includes the numbers of virtual zero-injection (ZI) measurements, complex power flow measurements (S), PMU current measurements (PMU_I), and PMU voltage measurements (PMU_V). The systems having the letter A have fewer PMU measurements than those with the letter B, and those with the letter B do not have complex power measurements. The percentage standard deviations of the measurements are given in Table II. The error is simulated under two distributions: Gaussian noise with zero mean and a per-unit standard deviation computed as a percentage of the full-scale meter reading, and an exponential noise distribution. The exponential noise is distributed according to the probability density function: $P(x|\lambda) = \lambda e^{-\lambda x}$, where λ is a parameter calculated from the standard deviation using $\lambda = \sqrt{\frac{1}{\sigma^2}}$. The Exponential distribution was chosen because it can be easily implemented in C++, and it is close to the Laplace distribution that was suggested in [38]. The weights usually are selected as one over the square of the per-unit standard deviation.

TABLE III
EXECUTION TIME AND SPEED-UP FACTOR (GAUSSIAN NOISE)

Net.	CECE (ms)	CTSE (ms)	CTSE SUF	PGNE (ms)	PGNE SUF
118A	4.0	1.04	3.85	0.3	13.3
118B	0.95	0.91	1.04	0.26	3.65
1888A	83.02	21.39	3.88	13.06	9.37
1888B	18.55	17.53	1.06	4.84	3.83
9241A	428.1	109.8	3.90	45.37	9.44
9241B	104.1	101.4	1.03	28.17	3.70

TABLE IV
MEASUREMENT ERROR AND ITERATION COUNT

Net.	Perf. Index ξ_z (pu)						Iter. #	
	Gaussian noise			Exponential noise			Gaussian noise	
	CECE	CTSE	PGNE	CECE	CTSE	PGNE	CECE	PGNE
118A	11.880	129.28	15.342	15.793	172.01	16.740	3	6
118B	22.564	28.501	27.296	27.801	34.004	31.533	1	1
1888A	32.340	3670.8	32.644	33.514	3944.1	34.022	4	8
1888B	19.840	46.849	18.662	21.248	47.910	20.982	1	1
9241A	23.589	3153.1	23.657	24.810	3544.2	26.056	5	11
9241B	10.313	35.652	10.018	12.529	42.736	12.044	1	1

Table III shows the computing time for the CECE [35], the CTSE [5], and the proposed PGNE. The table also shows the Speed-Up Factor (SUF) for the CTSE and the PGNE relative to the CECE, which forms the reference for execution time comparison. The results reveal that the PGNE gives a higher speed-up as compared to the CTSE, and the speed-up value is higher for the networks having complex power measurements (marked by the letter A, i.e., measurement scheme A). The SUF_PGNE is between 9.3 and 13.3 for the systems with complex power measurements, while the corresponding SUF_CTSE is around 4. Table IV reports the corresponding iteration counts and the values of the measurement error performance index as given by (32). As expected, there is no need for iterations for the systems without complex power measurements (scheme B). For systems with the measurement scheme A, the measurement error performance values for PGNE are significantly lower in comparison with CTSE. The conclusion holds for both Gaussian and Exponential measurement noise.

$$\xi_z = \sum_{i=1}^{m} \left| z_i^{estimated} - z_i^{true} \right|^2 \tag{32}$$

The test instances whose names end with the letter B do not have SCADA measurements; they make use only of PMU and ZI measurements, as Table I shows. Given that the PMU measurements have low errors (compared to SCADA), the results in

TABLE V
AVERAGE MEASUREMENT ERROR PER MEASUREMENT TYPE (GAUSSIAN NOISE)

Net.	Estimator	Average ξ_z (pu)		
		S	PMU_I	PMU_V
118A	CECE	0.0435	0.0200	0.0262
	CTSE	0.3807	0.3128	0.0984
	PGNE	0.0425	0.0399	0.0028
118B	CECE		0.1198	0.0023
	CTSE		0.1518	0.0022
	PGNE		0.1452	0.0024
1888A	CECE	0.0112	0.0032	$1.1 \cdot 10^{-4}$
	CTSE	1.2733	0.3547	0.0079
	PGNE	0.0112	0.0034	$8.9 \cdot 10^{-5}$
1888B	CECE		0.0078	$4.5 \cdot 10^{-5}$
	CTSE		0.0184	$1.1 \cdot 10^{-4}$
	PGNE		0.0078	$4.3 \cdot 10^{-5}$
9241A	CECE	0.0012	$4.9 \cdot 10^{-4}$	$4.6 \cdot 10^{-6}$
	CTSE	0.1637	0.0655	0.0032
	PGNE	0.0012	$4.9 \cdot 10^{-4}$	$4.8 \cdot 10^{-6}$
9241B	CECE		$6.4 \cdot 10^{-4}$	$3.4 \cdot 10^{-6}$
	CTSE		0.0022	$1.1 \cdot 10^{-5}$
	PGNE		$6.2 \cdot 10^{-4}$	$3.3 \cdot 10^{-6}$

TABLE VI
AVERAGE MEASUREMENT ERROR PER MEASUREMENT TYPE (EXPONENTIAL NOISE)

Net.	Estimator	Average ξ_z (pu)		
		S	PMU_I	PMU_V
118A	CECE	0.0448	0.0400	0.0025
	CTSE	0.4832	0.4411	0.0276
	PGNE	0.0470	0.0429	0.0027
118B	CECE		0.0920	0.0905
	CTSE		0.1560	0.0423
	PGNE		0.1581	0.0180
1888A	CECE	0.0117	0.0031	$1.9 \cdot 10^{-4}$
	CTSE	1.3626	0.3920	0.0107
	PGNE	0.0118	0.0033	$7.3 \cdot 10^{-5}$
1888B	CECE		0.0079	$7.2 \cdot 10^{-4}$
	CTSE		0.0178	$5.4 \cdot 10^{-7}$
	PGNE		0.0082	$6.4 \cdot 10^{-5}$
9241A	CECE	0.0013	$5.1 \cdot 10^{-4}$	$9.2 \cdot 10^{-6}$
	CTSE	0.1845	0.0726	0.0033
	PGNE	0.0014	$5.4 \cdot 10^{-4}$	$5.3 \cdot 10^{-6}$
9241B	CECE		$7.5 \cdot 10^{-4}$	$6.1 \cdot 10^{-5}$
	CTSE		0.0025	$2.4 \cdot 10^{-4}$
	PGNE		$7.3 \cdot 10^{-4}$	$3.5 \cdot 10^{-5}$

Table IV suggest that the use of the alternative complex measurement residuals (18) with PGNE results in a slight improvement in the performance index on the large test instances. The same trend is reflected in Table V and VI, which show a breakdown of the measurement errors averaged per measurement type.

In summary, the PGNE is faster than CECE [35], with a speed-up factor that is 7.2 on average and without an appreciable change in the accuracy. As compared to CTSE [5], PGNE is three times faster on average (average speed-up factor is 3.0), and it is much more accurate, especially when there is a steep change in load as the next section illustrates. The relative speed-up of PGNE is due to having a smaller size matrix that is factorized only once, and its accuracy is because the right-hand-side is iteratively updated until convergence.

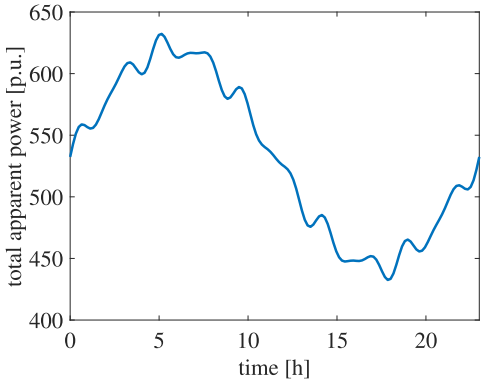

Fig. 2. Gradual change in total load.

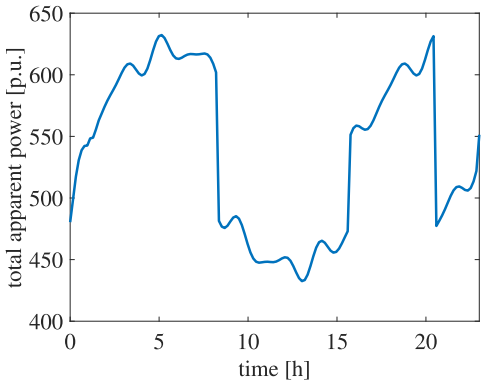

Fig. 3. Steep change in total load.

A. *Tracking Mode Operation*

The loads at all nodes were uniformly scaled to illustrate the operation of the estimator in tracking mode. Two load profiles were considered: a scenario with gradual change as in Fig. 2 and another with an abrupt change as in Fig. 3. Figs. 4–7 depict the logarithm of the measurement performance index in (32) for both load scenarios under Gaussian measurement noise, and when considering measurement schemes A and B of the 1888 network, following Table I. The figures consistently show the superiority of the PGNE as compared to the CTSE, as reflected by consistent lower measurement performance error values.

A concern linked to all hybrid state estimation implementations is the differing refresh speeds of PMU and SCADA systems, resulting in non-coincident measurements [32]; typically, PMU measurements are scanned at 30 samples per second, while SCADA measurements are recorded every 2 to 5 seconds. The outcome is that at every occurrence of the state estimator computation, a large number of phasor measurement values

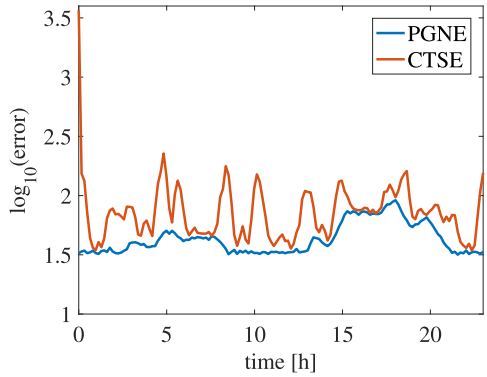

Fig. 4. Measurement error performance index – gradual change in load, 1888 A system.

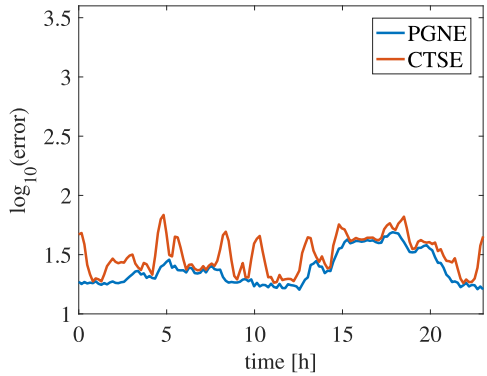

Fig. 5. Measurement error performance index – gradual change in load, 1888B system.

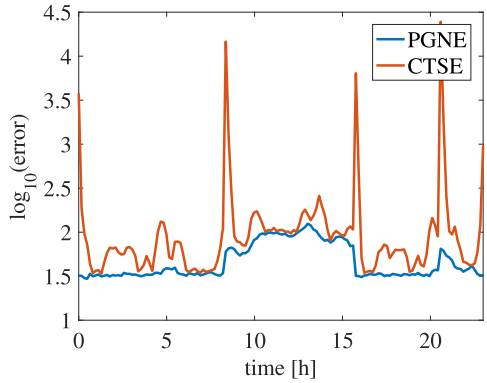

Fig. 6. Measurement error performance index – steep change in load, 1888 A system.

correspond to the current set of SCADA measurement values. One approach for handling the difference in the recording speeds between PMU and SCADA measurements is using buffering, which manages to distinguish the set of phasor measurement values to be used in the hybrid estimator solution [39], [40]. In the numerical experiments, the three estimators, i.e., PGNE, CECE, and CTSE, are assumed to use the most recently available measurements, whether they are SCADA or PMU.

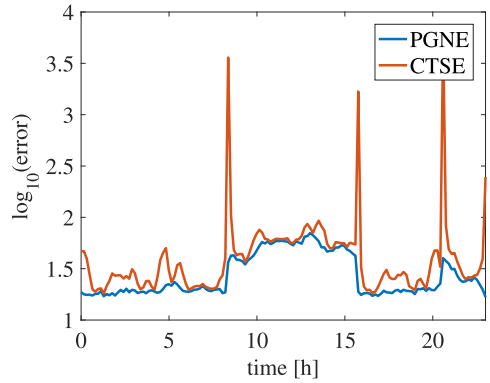

Fig. 7. Measurement error performance index – steep change in load, 1888B system.

TABLE VII
BAD DATA IDENTIFICATION STATISTICS – AVERAGE OVER 1000 MONTE-CARLO TRIALS (GAUSSIAN NOISE)

Bad measurement	Detection %		$\max(f_c^n)$	
	CTSE	PGNE	CTSE	PGNE
P	81.3	93.6	4.151	4.347
Q	80.4	93.2	4.066	4.264
S(P+Q)	85.7	100	5.367	5.786
PMU_I	85.2	90.4	3.922	4.164
PMU_V	85.8	95.3	3.057	3.086
S+PMU_I	91.2	100	4.682	4.993
S+PMU_V	90.7	100	3.211	3.283
PMU_I+PMU_V	95.2	100	3.266	3.321

B. Bad Data Identification

Table VII shows a comparison between the performance of the PGNE and the CTSE for Bad Data Identification (BDI) using the largest normalized residual test, as outlined in Section IV-B. Over 1000 trials of erroneous data amongst measurement types in the left column of Table VII, the second and third columns provide the percentage of successful detection when using the CTSE and the PGNE, respectively. The fourth and fifth column give the average of the $\max(f_c^n)$ in Step 5 of Section IV-B. The higher detection rate for the PGNE is attributed to the larger values of normalized residuals for bad data points.

C. Current Magnitude Measurements

Although transmission network state estimation does not usually make use of current magnitude measurements, there are cases where such measurements are useful for increasing redundancy or even ensuring observability at the sub-transmission level. Starting from the 1888 A system in Table I that has 2531 complex power flow measurements, some power flow measurements were replaced by branch current magnitude measurements to test the performance of the PGNE. Table VIII summarizes the results where the swapping of measurements is carried out in multiples of 5. The table shows the effect of using the complex power flow and current magnitude measurements as opposed to not considering the current magnitude measurements (i.e., using the number of complex power flow measurements in

TABLE VIII
IMPACT OF CURRENT MAGNITUDE MEASUREMENTS ON THE NUMBER OF ITERATIONS AND MEASUREMENT ERROR PERFORMANCE OF PGNE (1888 NODE NETWORK – GAUSSIAN NOISE)

Meas. #		Iter. #		Perf. Index ξ_z (pu)	
S_{KL}	$\lvert I_{KL}\rvert$	w/o $\lvert I_{KL}\rvert$	with $\lvert I_{KL}\rvert$	w/o $\lvert I_{KL}\rvert$	with $\lvert I_{KL}\rvert$
2526	5	8	8	32.5515	32.4777
2521	10	8	13	33.1515	32.8503
2516	15	9	11	32.6114	32.3181
2511	20	8	13	34.0295	33.5053
2506	25	8	12	31.5248	31.0632
2501	30	8	14	33.9032	33.2724
2496	35	8	14	30.0775	29.1949
2491	40	8	12	30.5968	29.7832
2486	45	9	15	34.7698	31.7914
2481	50	8	15	32.9697	30.5199

the first column). The results reveal that the use of current magnitude measurements in the PGNE increases the number of iterations. Still, the current magnitude measurements give a measurement performance error index (32) that has a value less than that obtained without using them. Table VIII does not show a comparison with the CTSE, as the details for handling current magnitude measurements were not reported in [5].

VI. CONCLUSION

This paper presented a new constant gain matrix method for hybrid state estimation. The technique is derived starting from the Perturbed Gauss-Newton (PGN) method and employs Wirtinger calculus to run entirely in the complex variable domain. The result of the derivation is an iterative approach that is essentially an extension of the implicit Z-bus power flow method to state estimation. The proposed PGN estimator is ideal for tracking mode operation. It is computationally efficient because it employs a single factorization of the coefficient matrix. The PGN method is validated through comparison with a recent complex variable equality constrained GN estimator [35], and it is shown to be superior to a two-stage complex variable estimator that does not involve iterations [5].

APPENDIX

This section describes the components of (18) for a measurement i, denoted by $[z_c(x,\overline{x})]_i$ and $[Hx]_i$, where x is the same as the vector U of nodal voltage phasors. The superscript M as used below denotes a measured quantity.

A. PMU Measurement – Voltage At Node K: U_K^M

$$[z_c(x,\overline{x})]_i = U_K^M \tag{33}$$

$$[Hx]_i = U_K \tag{34}$$

There are two approaches to modeling the reference angle condition [35]. In the first approach, a common GPS reference is used for all nodal voltages, and the slack node voltage measurement is modeled like any other PMU voltage measurement. In the second approach, a bus where a PMU is present is chosen as the reference; in this case, the slack angle condition is accounted for by having the angle of U_K^M being zero.

B. PMU Measurement – Branch Current From Node K to Node L: I_{KL}^M

$$[z_c(x,\overline{x})]_i = I_{KL}^M \tag{35}$$

$$[Hx]_i = Y_{KK}^P U_K + Y_{KL}^P U_L \tag{36}$$

where the superscript P in the admittance terms $Y_\bullet^P$ is to indicate that they are primitive values corresponding to the component, which in this case is the branch.

C. PMU Measurement – Current Injection At Node K: I_K^M

$$[z_c(x,\overline{x})]_i = I_K^M \tag{37}$$

$$[Hx]_i = Y_{KK}^S U_K + \sum_{L\in\varphi_K} Y_{KL}^S U_L \tag{38}$$

where the superscript S in the admittance terms $Y_\bullet^S$ is to indicate that they are system values, and φ_K is the set of nodes connected to node K by a branch. Note that the PMU current injection measurement is also used to model virtual zero-injection measurements as in (25), with $I_K^M = 0$.

D. SCADA Measurement – Branch Complex Power Flow From Node K to Node L: S_{KL}^M

$$[z_c(x,\overline{x})]_i = \frac{\overline{S}_{KL}^M}{\overline{U}_K} \tag{39}$$

$$[Hx]_i = Y_{KK}^P U_K + Y_{KL}^P U_L \tag{40}$$

E. SCADA Measurement – Complex Power Injection At Node K: S_K^M

$$[z_c(x,\overline{x})]_i = \frac{\overline{S}_K^M}{\overline{U}_K} \tag{41}$$

$$[Hx]_i = Y_{KK}^S U_K + \sum_{L\in\varphi_K} Y_{KL}^S U_L \tag{42}$$

F. SCADA Measurement – Voltage Magnitude At Node K: $\lvert U_K\rvert^M$

$$[z_c(x,\overline{x})]_i = |U_K|^M \angle \text{angle}\,(U_K) \tag{43}$$

$$[Hx]_i = U_K \tag{44}$$

G. SCADA Measurement – Branch Current Magnitude From Node K to Node L: $\lvert I_{KL}\rvert^M$

$$[z_c(x,\overline{x})]_i = |I_{KL}|^M \angle \text{angle}\left(Y_{KK}^P U_K + Y_{KL}^P U_L\right) \tag{45}$$

$$[Hx]_i = Y_{KK}^P U_K + Y_{KL}^P U_L \tag{46}$$

REFERENCES

[1] T. Yang, H. Sun, and A. Bose, "Transition to a two-level linear state estimator-part I: Architecture," *IEEE Trans. Power Syst.*, vol. 26, no. 1, pp. 46–53, Feb. 2011.

[2] L. Zhang, A. Bose, A. Jampala, V. Madani, and J. Giri, "Design, testing, and implementation of a linear state estimator in a real power system," *IEEE Trans. Smart Grid*, vol. 8, no. 4, pp. 1782–1789, Jul. 2017.

[3] A. Dubey, S. Chakrabarti, A. Sharma, and V. Terzija, "Optimal utilisation of PMU measurements in power system hybrid state estimators," *IET Gener. Transmiss, Distrib.*, vol. 13, no. 21, pp. 4978–4986, Nov. 2019.

[4] C. Gomez-Quiles, A. de la Villa Jaen, and A. Gomez-Exposito, "A factorized approach to WLS state estimation," *IEEE Trans. Power Syst.*, vol. 26, no. 3, pp. 1724–1732, Aug. 2011.

[5] A. S. Dobakhshari, S. Azizi, M. Paolone, and V. Terzija, "Ultra fast linear state estimation utilizing SCADA measurements," *IEEE Trans. Power Syst.*, vol. 34, no. 4, pp. 2622–2631, Jul. 2019.

[6] G. H. Couch, "Improved power system state estimation with constant gain matrices," in *Proc. IEEE*, vol. 64, no. 11, Nov. 1976, pp. 1641–1643.

[7] H. P. Horisberger, J. C. Richard, and C. Rossier, "A fast decoupled static state-estimator for electric power systems," *IEEE Trans. Power Appar. Syst.*, vol. 95, no. 1, pp. 208–215, Jan./Feb. 1976.

[8] S. Gratton, A. S. Lawless, and N. K. Nichols, "Approximate Gauss-Newton methods for nonlinear least squares problems," *SIAM J. Optim.*, vol. 18, no. 1, pp. 106–132, 2007.

[9] W. Wirtinger, "Zur formalen theorie der funktionen von mehr komplexen veranderlichen," *Mathematische Annalen*, vol. 97, pp. 257–376, 1927.

[10] K. Kreutz-Delgado, "The complex gradient operator and the CR-calculus," 2009. [Online]. Available: http://arXiv.org/abs/0906.4835.

[11] B. Stott, "Review of load-flow calculation methods," in *Proc. IEEE*, vol. 62, no. 7, Jul. 1974, pp. 916–929.

[12] T. H. Chen, M. S. Chen, K. J. Hwang, P. Kotas, and E. A. Chebli, "Distribution system power flow analysis-a rigid approach," *IEEE Trans. Power Del.*, vol. 6, no. 3, pp. 1146–1152, Jul. 1991.

[13] T. Yang, H. Sun, and A. Bose, "Transition to a two-level linear state estimator-Part II: Algorithm," *IEEE Trans. Power Syst.*, vol. 26, no. 1, pp. 54–62, Feb. 2011.

[14] M. Göl and A. Abur, "LAV based robust state estimation for systems measured by PMUs," *IEEE Trans. Smart Grid*, vol. 5, no. 4, pp. 1808–1814, Jul. 2014.

[15] M. Göl and A. Abur, "A fast decoupled state estimator for systems measured by PMUs," *IEEE Trans. Power Syst.*, vol. 30, no. 5, pp. 2766–2771, Sep. 2015.

[16] J. Lin *et al.*, "A robust complex-domain state estimator using synchrophasor measurements," *Int. J. Elect. Power Energy Syst.*, vol. 96, pp. 412–421, Mar. 2018.

[17] T. Bi, X. Qin, and Q. Yang, "A novel hybrid state estimator for including synchronized phasor measurements," *Elec. Power Syst. Res.*, vol. 78, no. 8, pp. 1343–1352, Aug. 2008.

[18] G. Valverde, S. Chakrabarti, E. Kyriakides, and V. Terzija, "A constrained formulation for hybrid state estimation," *IEEE Trans. Power Syst.*, vol. 26, no. 3, pp. 1102–1109, Aug. 2011.

[19] A. Garcia, A. Monticelli, and P. Abreu, "Fast decoupled state estimation and bad data processing," *IEEE Trans. Power Appar. Syst.*, vol. PAS-98, no. 5, pp. 1645–1652, Sep. 1979.

[20] A. Monticelli and A. Garcia, "Fast decoupled state estimators," *IEEE Trans. Power Syst.*, vol. 5, no. 2, pp. 556–564, May 1990.

[21] J. J. Allemong, L. Radu, and A. M. Sasson, "A fast and reliable state estimation algorithm for AEP's new control center," *IEEE Trans. Power Appar. Syst.*, vol. PAS-101, no. 4, pp. 933–944, Apr. 1982.

[22] A. Gómez-Expósito, C. Gómez-Quiles, and A. de la Villa Jaén, "Bilinear power system state estimation," *IEEE Trans. Power Syst.*, vol. 27, no. 1, pp. 493–501, Feb. 2012.

[23] C. Gómez-Quiles, H. A. Gil, A. de la Villa Jaén, and A. Gómez-Expósito, "Equality-constrained bilinear state estimation," *IEEE Trans. Power Syst.*, vol. 28, no. 2, pp. 902–910, May 2013.

[24] Y. Chen, F. Liu, S. Mei, and J. Ma, "Mixed integer linear programming formulation for robust state estimation," in *Proc. IEEE PES Innov. Smart Grid Technol., Eur.*, 2014, pp. 1–4.

[25] B. Fardanesh, "Direct non-iterative power system state solution and estimation," in *Proc. IEEE Power Energy Soc. Gen. Meeting*, 2012, pp. 1–6.

[26] X. T. Jiang, B. Fardanesh, D. Maragal, G. Stefopoulos, J. H. Chow, and M. Razanousky, "Improving performance of the non-iterative direct state estimation method," in *Proc. Power Energy Conf. Illinois*, 2014, pp. 1–6.

[27] X. T. Jiang, J. H. Chow, B. Fardanesh, D. Maragal, G. Stefopoulos, and M. Razanousky, "Power system state estimation using a direct non-iterative method," *Int. J. Elec. Power Energy Syst.*, vol. 73, pp. 361–368, Dec. 2015.

[28] A. Jovicic, M. Jereminov, L. Pileggi, and G. Hug, "An equivalent circuit formulation for power system state estimation including PMUs," in *Proc. North Amer. Power Symp.*, 2018, pp. 1–6.

[29] M. R. Wagner, M. Jereminov, A. Pandey, and L. Pileggi, "A probabilistic approach to power system state estimation using a linear algorithm," in *Proc. IEEE Int. Conf. Environ. Elect. Eng. Ind. Commercial Power Syst. Eur.*, 2019, pp. 1–6.

[30] A. Jovicic, M. Jereminov, L. Pileggi, and G. Hug, "A linear formulation for power system state estimation including RTU and PMU measurements," in *Proc. IEEE PES Innov. Smart Grid Technol. Eur.*, 2019, pp. 1–5.

[31] B. Stott and O. Alsac, "Fast decoupled load flow," *IEEE Trans. Power Appar. Syst.*, vol. PAS-93, no. 3, pp. 859–869, May 1974.

[32] I. Džafić, R. A. Jabr, and T. Hrnjić, "Hybrid state estimation in complex variables," *IEEE Trans. Power Syst.*, vol. 33, no. 5, pp. 5288–5296, Sep. 2018.

[33] R. A. Jabr and B. C. Pal, "Iteratively reweighted least-squares implementation of the WLAV state-estimation method," in *Proc. IEE - Gener. Transmiss Distrib.*, vol. 151, no. 1, pp. 103–108, 2004.

[34] A. Abur and A. Gómez Expósito, *Power System State Estimation: Theory and Implementation*. New York, NY, USA: Marcel Dekker, 2004.

[35] I. Džafić and R. A. Jabr, "Real-time equality-constrained hybrid state estimation in complex variables," *Int. J. Elec. Power Energy Syst.*, vol. 117, May 2020, Art. no. 105634.

[36] C. Josz, S. Fliscounakis, J. Maeght, and P. Panciatici, "AC power flow data in MATPOWER and QCQP format: iTesla, RTE snapshots, and PEGASE," 2016, *arXiv:1603.01533*.

[37] R. D. Zimmerman, C. E. Murillo-Sánchez, and R. J. Thomas, "Matpower: Steady-state operations, planning, and analysis tools for power systems research and education," *IEEE Trans. Power Syst.*, vol. 26, no. 1, pp. 12–19, Feb. 2011.

[38] S. Wang, J. Zhao, Z. Huang, and R. Diao, "Assessing Gaussian assumption of PMU measurement error using field data," *IEEE Trans. Power Del.*, vol. 33, no. 6, pp. 3233–3236, Dec. 2018.

[39] Y. Chakhchoukh, V. Vittal, and G. T. Heydt, "PMU based state estimation by integrating correlation," *IEEE Trans. Power Syst.*, vol. 29, no. 2, pp. 617–626, Mar. 2014.

[40] V. Murugesan, Y. Chakhchoukh, V. Vittal, G. T. Heydt, N. Logic, and S. Sturgill, "PMU data buffering for power system state estimators," *IEEE Power Energy Tech. Syst. J.*, vol. 2, no. 3, pp. 94–102, Sep. 2015.

Izudin Džafić (Senior Member, IEEE) received the Ph.D. degree from the University of Zagreb, Zagreb, Croatia, in 2002. He is currently a Professor with the Department of Automatic Control and Electronics, Faculty of Electrical Engineering, University of Sarajevo, Bosnia and Herzegovina. From 2002 to 2014, he was with Siemens AG, Nuremberg, Germany, where he held the position of the Head of the Department and Chief Product Owner (CPO) for Distribution Network Analysis (DNA) R&D. He holds eight US and international patents. His research interests include power system modeling, development and application of fast computing to power systems simulations. He is a member of the IEEE Power and Energy Society and the IEEE Computer Society.

Rabih A. Jabr (Fellow, IEEE) was born in Lebanon. He received the B.E. degree in electrical engineering (with high distinction) from the American University of Beirut, Beirut, Lebanon, in 1997, and the Ph.D. degree in electrical engineering from Imperial College London, London, U.K., in 2000. He is currently a Professor with the Department of Electrical and Computer Engineering, American University of Beirut. His research interests are in mathematical optimization techniques and power system analysis and computing.

Tarik Hrnjić (Student Member, IEEE) received the B.Sc. and M.Sc. degrees in electrical engineering from the International University of Sarajevo, Bosnia and Herzegovina, in 2015 and 2016, respectively. He is currently an Assistant with the Department of Computer Science and Informatics, University of Sarajevo, Bosnia. His research interests include analysis and optimization of power systems.